

Quantum Monte Carlo study of strongly interacting Fermi gases

Stefano Gandolfi

Theoretical Division, Los Alamos National Laboratory Los Alamos, NM 87545, USA

E-mail: stefano@lanl.gov

Abstract. In recent years Quantum Monte Carlo techniques provided to be a valuable tool to study strongly interacting Fermi gases at zero temperature. We have used QMC methods to investigate several properties of the two-components Fermi gas at unitarity and in the BCS-BEC crossover, both with equal and unequal masses corresponding to the $Li-K$ Fermi mixture. In this paper we present several recent QMC results, including the energy at zero and finite effective range, the contact parameter and the static structure factor, which, at low momentum, depends strongly on the phonons in the unitary Fermi gas.

1. Introduction

During the last years important efforts have been devoted to study ultra-cold Fermi gases, both experimentally and theoretically (for a review see for example Ref. [1]). By means of Feshbach resonance it is possible experimentally to adjust the interaction between atoms. The system can be tuned to a BCS state where Fermions are weakly interacting, to the so called unitary regime where the two-body scattering length is infinite, or to form a BEC condensate of Bosons. Theoretically, ultra-cold Fermi gases have become an important testing ground for a host of many-body methods, as well as an avenue to studying new physics.

The study of ultra-cold Fermi gases is very intriguing, and the unitary limit became a very interesting many-body problem to solve for several reasons. These systems can be experimentally studied at very low temperatures of the order of $0.1 T_F$, essentially zero temperature. They are very dilute, and their properties are independent of the form of the Hamiltonian used to describe the system, the results given by any model satisfying the limits of large scattering length and small effective range must be identical. Moreover these systems are very strongly interacting, methods based on perturbation theory, mean-field, or expansions of small parameters are not obviously convergent, and the calculation of the properties of the Unitary Fermi gas is very challenging. The properties scale with powers of the Fermi momentum $k_F = (3\pi^2\rho)^{1/3}$. The interparticle separation r_0 is approximately given by $r_0 = (9\pi/4)^{1/3}/k_F$, and the dilute regime is guaranteed by imposing $r_0 \gg r_e$, where r_e is the effective range of the two-body interaction. The universal regime is given when $r_e \ll r_0 \ll a$, where a is the scattering length, and the unitary limit correspond to the case of $|a| = \infty$. In the limit of $r_e = 0$ the only scale of the system is

r_0 or more conveniently the Fermi momentum k_F . Thus a natural unit for the energy if given by the Fermi-gas energy $E_{FG} = 3\hbar^2 k_F^2 / 10m$, and there are no other free parameters. For this reason, these systems are called universal.

Ultra-cold Fermi gases can also be realized with population imbalance, and the system can eventually exhibit different phases [2, 3] where superfluid and normal phases may coexist or phase separate [4, 5], or other intriguing more exotic phases like LOFF or p -wave superfluidity could appear [6, 7]. In the last few years a new direction of research has been undertaken: the realization of trapped two-component Fermi gases with the mixture of Fermions with different masses, in particular the ${}^6\text{Li}-{}^{40}\text{K}$ mixture has been addressed [8–10]. The properties of systems with mass imbalance can be very different from the equal masses case; for example, for majority light population the Chandrasekhar–Clogston limit is very small and close to zero [11]. Then, at unitarity, the two-components Fermi gas with different masses may exhibit very different properties with respect to the equal mass case [12, 13], even in the BCS limit [14].

Several predictions for equal mass Fermi gases were made possible through Quantum Monte Carlo techniques (QMC), later confirmed by experiments [4, 11, 15–21]. The Variational Monte Carlo (VMC) and the Diffusion Monte Carlo (DMC) enable accurate calculations of the ground state of strongly interacting Fermions at unitarity, and to study its properties [20]. In addition, the unbalanced two-component Fermi gases with equal masses do not exhibit a sign problem using the Auxiliary Field Monte Carlo (AFMC) [21], and this permits a very accurate calculation to benchmark other many-body calculations. Experiments are possible at very low temperatures of the order of fractions of T_F , and then the zero temperature properties can be directly obtained from experiments.

In this paper we will review several properties calculated using QMC methods, including the exact calculation of the energy, the role of the effective range, the BCS-BEC crossover, and other properties including the contact parameter and the static structure factor.

2. The model and QMC methods

The AFMC performed on a lattice through the use of auxiliary fields does not suffer of the Fermion sign problem and permits to calculate exactly the energy of the unpolarized Fermi gas [21]. The AFMC method uses a BCS wave function as a trial wave function. In this section we describe the variational wave function and the DMC method in the continuum.

In our study we model the ground state of the system in the continuum using the Hamiltonian

$$H = \sum_{i=1}^{N_l} \frac{-\hbar^2}{2m_l} \nabla_i^2 + \sum_{j=1}^{N_h} \frac{-\hbar^2}{2m_h} \nabla_j^2 + \sum_{i,j} v(r_{ij}), \quad (1)$$

where N_l and N_h is the number of particles with mass m_l and m_h . Since we want to model a system that is dilute, particles interact only in s -wave, and the potential v_{ij} is non-zero only between particles with opposite spin state or with different mass. Several forms of the potential v_{ij} has been explored, and provided to be equivalent in the limit of small effective range [22]. In most of our studies we have used the Pöschl-Teller already employed in several previous QMC calculations [11, 15, 17, 19, 20, 22–25]:

$$v(r) = -v_0 \frac{\hbar^2}{m_r} \frac{\mu^2}{\cosh^2(\mu r)}, \quad (2)$$

where m_r is the reduced mass, and the parameters μ and v_0 tune respectively the effective range r_e and the scattering length a of the interaction. For this potential, the unitary limit

corresponding to the zero-energy ground state between two particles is with $v_0 = 1$ and $r_e = 2/\mu$. Most of the results presented in this work have been obtained by fixing $r_e k_F \approx 0.03$ but in several cases we considered different values to check effects due to the effective range of the potential. It is also possible to use other forms of the potential $v(r)$, and the results are universal in the limit of small effective range as we shall discuss in the next sections.

The QMC calculations are performed using the Jastrow-BCS form of the wave function of Refs. [15, 20]:

$$\Psi_v(\mathbf{r}_1 \dots \mathbf{r}_N) = F(\mathbf{r}_1 \dots \mathbf{r}_N) \Phi_{\text{BCS}}. \quad (3)$$

The antisymmetric part Φ_{BCS} is a particle-projected BCS wave function including pairing correlations. It is given by

$$\Phi_{\text{BCS}} = \mathcal{A}[\phi(r_{11'})\phi(r_{22'})\dots\phi(r_{nn'})]. \quad (4)$$

The operator \mathcal{A} is an anti-symmetrization operator, the unprimed coordinates are for spin-up or heavy particles and the primed are for spin-down or light particles, and $n = N/2$ for the unpolarized case. The pairing function is parametrized as

$$\begin{aligned} \phi(\mathbf{r}) &= \sum_n \alpha_{k_n^2} \exp[i\mathbf{k}_n \cdot \mathbf{r}] + \beta(r), \\ \beta(r) &= \tilde{\beta}(r) + \tilde{\beta}(L-r) - 2\tilde{\beta}(L/2), \\ \tilde{\beta}(r) &= [1 + cbr] [1 - \exp(-dbr)] \frac{\exp(-br)}{dbr}. \end{aligned} \quad (5)$$

In the infinite volume limit $\phi(\mathbf{r})$ is a function of one scalar variable, the product $k_F r$. The simulations use periodic boundary conditions in a finite volume. In this finite volume, the function $\beta(r)$ has a range of $L/2$, L is the size of the simulation box, the value of c is chosen such that $\beta(r)$ has zero slope at the origin, and b , d and $\alpha_{k_m^2}$ are variational parameters. Note that if $\beta(r) = 0$, and $\alpha_{k_m^2} = 0$ for $k > k_F$, $\Phi_{\text{BCS}} = \Phi_{FG}$, where the latter is the wave function describing the non interacting Fermi gas in the normal phase. As Φ_{FG} and Φ_{BCS} are orthogonal, we can study the Fermi gases both in the superfluid and in the normal phase [4, 5, 11]. The pairing wave function used here contains several free parameters that have been optimized by minimizing the energy of the system using VMC and following the strategy of Ref. [26]. In the BEC side of the transition, when $1/a k_F \geq 2$, we found that using the pairing function as described in Ref. [16], i.e. the two-body wave function instead of the function of Eq. 5, gives lower energies. Instead, in the BCS case for $1/a k_F \leq -1$, the BCS wave function Φ_{BCS} gives almost the same energy of Φ_{FG} as the pairing becomes less important to the equation of state. The polarized systems can be simulated by extending the wave function to include single-particle states for the unpaired particles [15, 23]. Note that the wave function previously described cannot reproduce more exotic phases like LOFF or p -wave pairing.

The Jastrow $F(R)$ includes a short- and a long-range part. The short-range term is given by

$$F_{sr}(R) = \prod_{i < j} f_{sr}(r_{ij}), \quad (6)$$

where the function $f_{sr}(r)$ acts only between particles with different spin or mass, and it is obtained by solving the equation

$$-\frac{\hbar^2}{2m_r} \nabla^2 f_{sr}(r) + \alpha v(r) f_{sr}(r) = \lambda f_{sr}(r). \quad (7)$$

The parameter λ is obtained by imposing the boundary condition $f(r > d_0) = 1$, where the healing distance d_0 is a variational parameter, and the quenching α is adjusted to be less than one only in the BEC regime. The correct boundary conditions to the wave function are guaranteed by constraining $d_0 \leq L/2$ where L is the size of the simulation box, but we found that a typical good choice is given by taking $d_0 \approx L/10$. By solving Eq. 7 we also assure the correct behavior of the wave function at small distances so that the Jastrow function f is defined to have $\partial f/\partial r=0$ at the origin. The calculation in the deep BEC can be also improved by adding a short-range function $f_{sr}(r)$ between particles with same spin or mass, and solving the equation above with a repulsive interaction.

In order to precisely calculate the static structure function at low momenta, it is important to include the effect of phonons as long-distance correlations. In our calculation, we include a term

$$F_{tr}(R) = \prod_{i<j} \exp \left[\gamma \sum_n \frac{\exp(-\beta|\mathbf{q}_n|)}{|\mathbf{q}_n|} \exp(-i\mathbf{q}_n \cdot \mathbf{r}_{ij}) \right], \quad (8)$$

where γ and β are new variational parameters [27]. The VMC algorithm is then used to optimize over wave functions of this form. Diffusion Monte Carlo (DMC) is then used to project out the ground state from:

$$\Phi_0 = \lim_{\tau \rightarrow \infty} \Psi(\tau), \quad (9)$$

where

$$\Psi(\tau) = e^{-(H-E_T)\tau} \Psi(0) = e^{-(H-E_T)\tau} \Psi_v. \quad (10)$$

The factor E_T is a constant used to control the normalization of the ground state. The propagation is achieved using a many-body propagator defined as

$$G(R', R, \delta\tau) = \langle R' | e^{-H\delta\tau} | R \rangle, \quad (11)$$

and

$$\Psi(R', \tau + \delta\tau) = \int dR G(R', R, \delta\tau) \Psi(R, \tau). \quad (12)$$

A good approximation of G can be obtained using a Trotter expansion, and iterating the above equation for small values of $\delta\tau$. Note that for a zero-range interaction the exact two-body propagator could also be used to sample the many-body Green's function [28]. In the case of Fermions there is a sign problem that needs to be taken care. A common approach combined with the DMC method is the fixed-node approximation. The sampling of paths is restricted to regions where the trial wave function is positive, and the problem is then recasted into a Bosonic problem (without sign problem) in a restricted subspace. This approximation results in providing an upper bound to the exact energy of the system, whose accuracy depends to the quality of the variational wave function. More details on the implementation of the VMC and DMC algorithms can be found in Ref. [29].

3. The BCS-BEC crossover and the unitary limit

The BCS-BEC crossover has been calculated extensively over the past ten years. The unitary limit is very interesting because perturbative methods cannot be applied. In addition, there are no small parameters to expand, and thus using numerical calculations is the only way to accurately explore the properties of the system. The energy of these systems is given by

$$E = \xi E_{FG}, \quad (13)$$

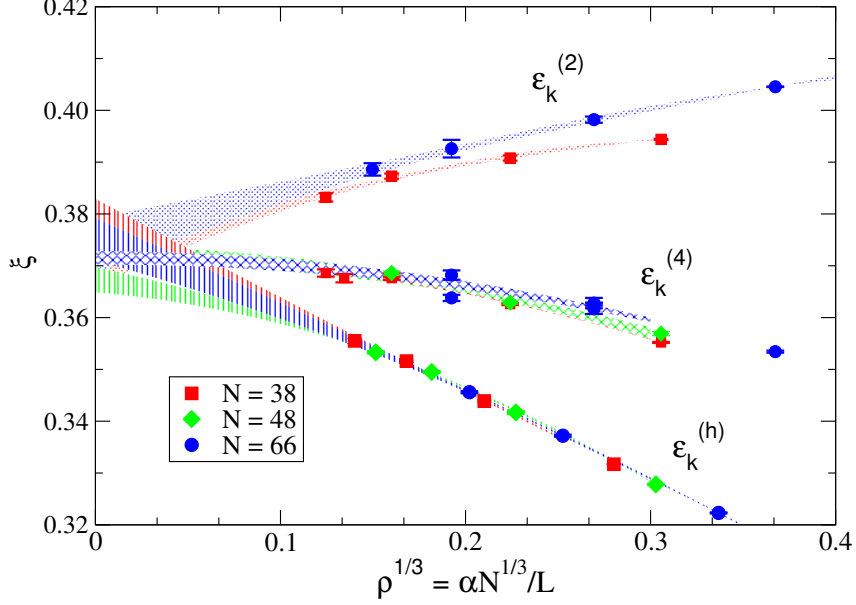


Figure 1. Ground state energy of the unitary Fermi gas calculated using the AFMC method. We show the value of ξ as a function of the lattice size for various particle numbers N and Hamiltonians, α is the lattice spacing. See Ref. [21] for more details.

where ξ is called Bertsch parameter. There have been several calculations of ξ based on QMC techniques, and recently we used the AFMC method to calculate exactly the energy of the system [21], the results are summarized in Fig. 1. Since the lattice space provides a natural regularization of the Hamiltonian, it is possible to test different models of kinetic energy or dispersion relations. In the figure, we show the results obtained using different regularization of the kinetic energy. All the results correspond the case of infinite scattering length, and in the case of $\epsilon_k^{(h)}$ and $\epsilon_k^{(2)}$, the results are obtained at finite values of effective range and need to be extrapolated. Results obtained using different number of particles are included in the figure. We note that finite size effects are basically absent, as using 38, 48 or 66 Fermions yields to the same energy. This fact is because the interaction is very short-range, and because pairing of the system is very strong. Particles behave like Bosons, and finite size effects associated to the kinetic energy vanish. The absence of sizeable finite size effects for more than ~ 40 particles has been also shown with a DMC calculation [25]. By extrapolating the results to zero effective range gives the result of $\xi = 0.372(5)$ [28] that is in excellent agreement with a subsequent experiment performed at MIT [30]. The best upper bound estimate using the fixed-node DMC method is $\xi = 0.389(1)$ [22].

Another quantity of interest is the dependence of the energy to the effective range:

$$\xi = \xi_0 + s k_{Fr} e + \dots \quad (14)$$

At unitarity the parameter s has been calculated using DMC and AFMC, and the different calculations yield $s = 0.11(3)$ and $s = 0.12(2)$ [21, 22]. In Fig. 2 we show the results obtained using DMC with various potentials for the equal mass case, and for a mass ratio $m_h/m_l = 6.5$ corresponding to the $Li - K$ mixture. It is pretty interesting that the value of s does not depend to the mass ratio of the two species.

The knowledge of the energy dependence to the effective range is important to compare

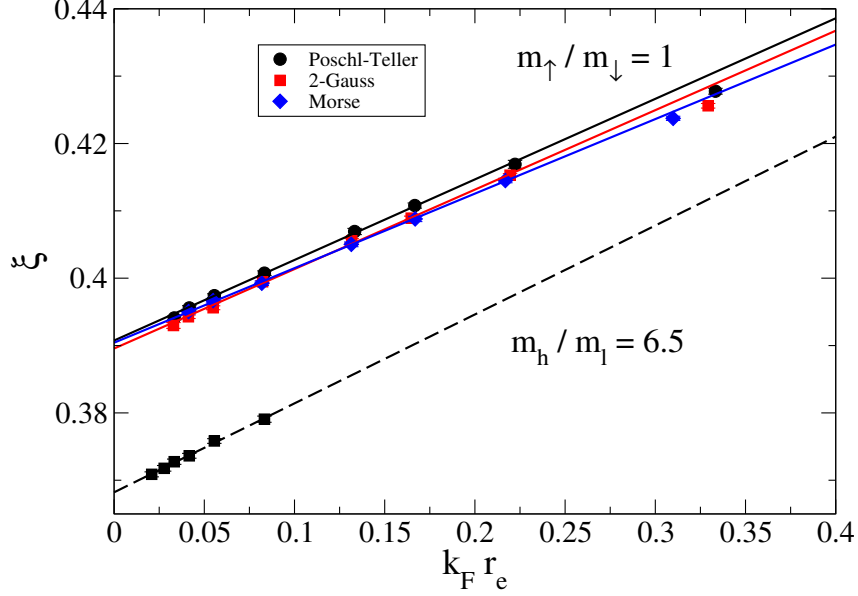


Figure 2. The value of ξ as a function of $k_F r_e$ calculated using DMC for the two-components with equal and unequal masses unitary Fermi gas. In the case of equal masses, the results obtained using different two-body potentials are presented. See Ref. [22] for more details.

properties of neutron matter and cold atoms. At low-densities, neutron matter has similar properties to cold atoms: the interaction is mainly s -wave, the effective range is small, and the scattering length is large [31]. In order to make qualitative comparisons between cold atoms and neutron matter it is important to take into account the fact that the neutron-neutron interaction has a small but finite r_e . Using the estimate of s as a function of $a k_F$ opens the possibility to compare these two different systems. An example of this comparison is reported in Fig. 3. In the figure we compare the cold atoms results corresponding to $r_e = 0$, the neutron matter equation of state calculated using the s -wave component of realistic nuclear forces [31, 32], and the results obtained by extrapolating the cold-atoms results to the effective range of neutron-neutron potential using Eq. 14.

In the BCS-BEC crossover, the two limits correspond to the BCS where Fermions are weakly attractive and to the BEC regime with very strong coupling. In the weak coupling limit, the energy of the interacting Fermi gas is given by [33]

$$\frac{E}{E_{FG}} = 1 + \frac{10}{9\pi} a k_F + \frac{4(11 - 2 \log 2)}{21\pi^2} (a k_F)^2 + \dots, \quad (15)$$

where a is the scattering length and k_F is the Fermi momentum of the system. In the very strong coupling limit, when $a k_F \rightarrow 0^+$, the system becomes made of Bosonic molecules, formed by one spin-up or heavy and one spin-down or light Fermion, that are weakly repulsive. Their energy is given by [34]

$$\frac{E/N - E_2/2}{E_{FG}} = \frac{10}{9\pi} a_{dd} k_F \frac{m_h m_l}{(m_h + m_l)^2} \times \left[1 + \frac{128}{15\sqrt{6}\pi^3} (a_{dd} k_F)^{3/2} + \dots \right], \quad (16)$$

where a_{dd} is the Boson-Boson scattering length that can be obtained from a few-body calculation [35], or even by fitting QMC results [16]. The BCS-BEC crossover for a two-component $Li - K$ Fermi-Fermi mixture is shown in Fig. 4. In the figure, the blue and black

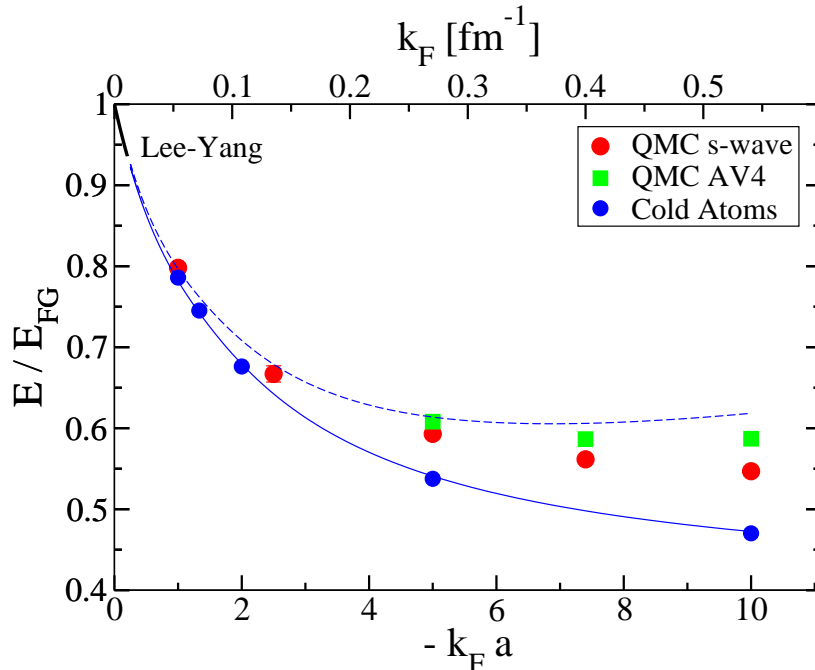


Figure 3. The equation of state of cold atoms and low-density neutron matter. For the latter, we show results obtained from the s -wave part of a realistic neutron-neutron potential, and those obtained by extrapolating the cold-atoms results to large effective ranges. See the text for details. This figure is taken from Ref. [28].

points correspond to the QMC results obtained using two different values of r_e in the two-body interaction. In the unitary limit, the energy can be expanded as

$$\frac{E}{E_{FG}} = \xi - \frac{\zeta}{a k_F} - \frac{5\nu}{3(a k_F)^2} + \dots \quad (17)$$

The fit to QMC results, extrapolated to $r_e = 0$, gives $\xi = 0.3726(6)$, $\zeta = 0.900(2)$ and $\nu = 0.46(1)$. The values of ζ and ν are very similar to the case of equal masses reported in Ref. [20]. In Fig. 4 we also show the two limits given by Eq. 15 and 16 that agree with the QMC results. The crossover corresponding to the $Li - K$ mixture is qualitatively similar to the equal masses case [16, 23].

4. Contact parameter and the static structure factor

One of the most intriguing properties of strongly interacting Fermi gases is the contact parameter. Shina Tan showed that several quantities, including the pair distribution function, momentum distribution, and the static structure factor in the limit of small distances or high momenta are fully described by the contact parameter [36–38]. Also the equation of state is related to the contact parameter. This particular property is very interesting because the contact can be calculated in different ways, and, more important, can be measured in different experiments (see for example Refs. [39–41]).

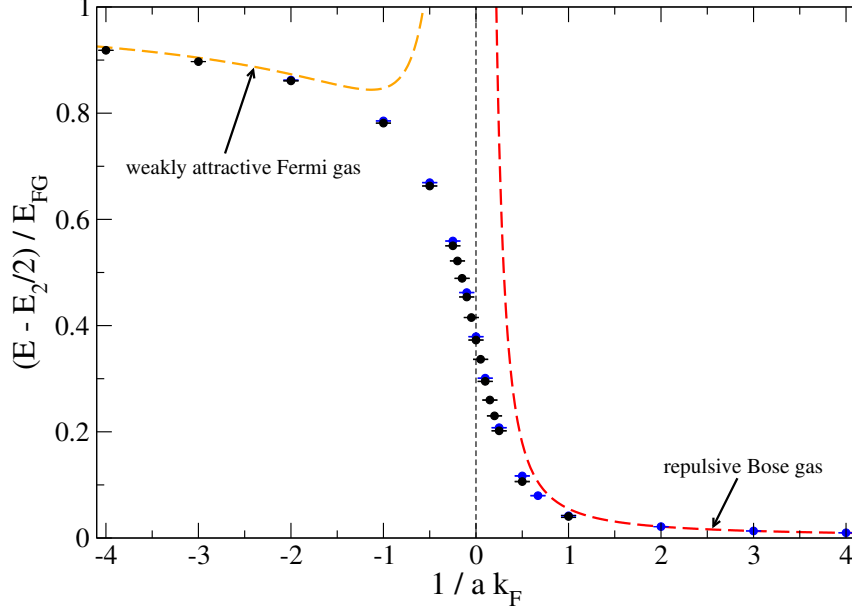


Figure 4. The BCS-BEC crossover calculated using DMC for the two-component unequal masses case corresponding to the $Li - K$ mixture. The two different set of points correspond to the results obtained using different values of r_e . The dashed lines correspond to the perturbative calculation of weakly attractive Fermi gas in the BCS, and of the weakly repulsive Bose gas in the BEC.

In Ref. [20] several observables related to the contact have been calculated using QMC methods. We note that, apart the fixed-node approximation, any other observable depends to the choice of Ψ_v . Within DMC, we have computed observables with

$$\langle O \rangle = 2O_m - O_V, \quad (18)$$

where

$$O_m = \langle \Phi_0 | O | \Psi_v \rangle, \quad (19)$$

and

$$O_V = \langle \Psi_v | O | \Psi_v \rangle. \quad (20)$$

Note that the energy is a special case, because the operator H commutes with the propagator G , and in this case it's easy to see that $\langle H \rangle = H_m$. The fact that several operators basically describe the same contact parameter is a proof of Tan's relations but also of the very good quality of the trial wave function employed in our calculations.

We have calculated the contact parameter in the BCS-BEC crossover using the adiabatic relation that relates the contact to the equation of state:

$$\frac{C}{Nk_F} = -\frac{6\pi}{5} \frac{\partial \xi}{\partial (k_F a)^{-1}}. \quad (21)$$

The contact parameter is shown in Fig. 5, and compared with recent measurements and with the result obtained by Enss *et al.* [42]. In the inset we show the equation of state. The experimental measurements based on the Bragg spectroscopy are in a very good agreement with our calculations, both at unitarity and in the BEC limit [43].

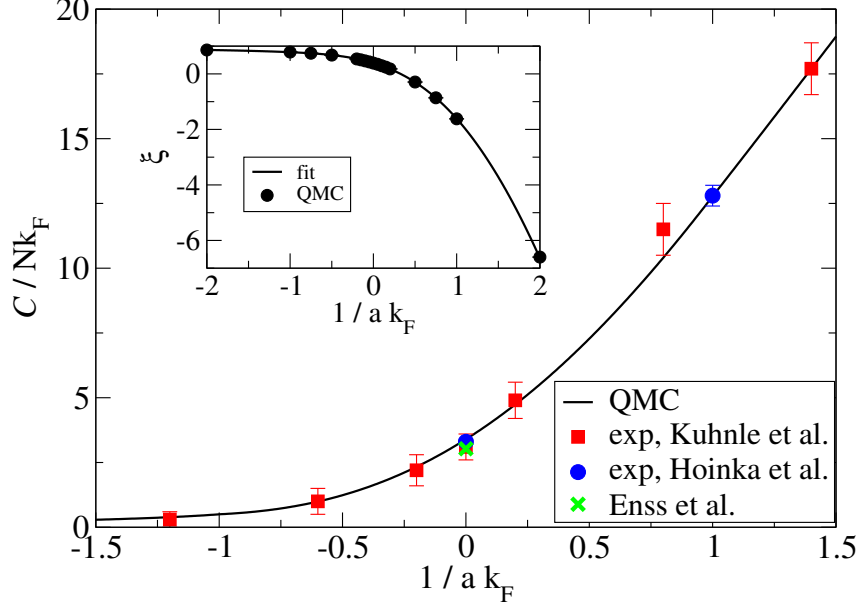


Figure 5. The contact parameter as a function of $1/a k_F$ obtained from the equation of state calculated using DMC (shown in the inset). The experimental points of Refs. [43, 44] and the result of Ref. [42] are also shown.

One of the quantities related to the contact is the static structure factor $S(q)$, that corresponds to the sum-rule of the density-response function:

$$S(q) = \int d\omega S(\omega, q). \quad (22)$$

The density-response function $S(\omega, q)$ has been measured by means of the Bragg spectroscopy [43, 45, 46]. At high momenta, this quantity is related to the contact through the relation

$$\frac{C}{Nk_F} = \frac{4q}{k_F} \left[\frac{S(q) - 1}{1 - 4/(\pi q a)} \right]. \quad (23)$$

At low momenta $S(q)$ is related to the long-wavelength phonons in the system. The quantity $S(q)$ has been calculated using QMC for different values of $a k_F$ in Ref. [43], and the agreement with experimental data is within 1%. The calculation of $S(q)$ at small q requires extra care. Due to the phonon dispersion, we found it very important to include long-range correlations in the variational wave function as discussed in Sec. 2. In Fig 6 we show the VMC results for $S(q)$ obtained by including (or not) the long range correlations in the Jastrow. We note that when the DMC algorithm is also used, the expectation value of $S(q)$ is less dependent to the presence of long-range correlations though even in this case the accuracy of the calculated $S(q)$ is much greater with the improved trial function. It would be very interesting to measure the behavior of $S(q)$ at small momenta, where collective modes are expected to be important.

5. Conclusions

In this paper we present recent results obtained using QMC methods for two-component strongly interacting Fermi gases. The energy and its dependence on the product of the effective range

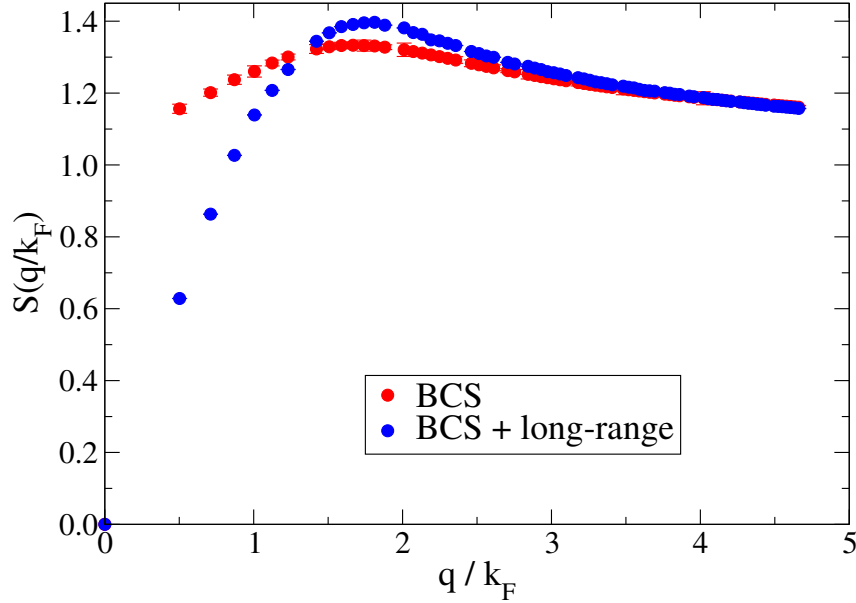


Figure 6. The static structure factor (density-response sum rule) as a function of q . The results have been obtained with the VMC, with and without long-range correlations in the Jastrow.

and Fermi momentum have been precisely determined theoretically and compared to experiment across the BCS-BEC crossover. Other properties related to the contact have also been computed, in particular the static structure factor, and the results are in very good agreement with experimental data. Future directions include dynamic response of the unitary Fermi gas, inhomogeneous systems and the transitions from three- to two-dimensions, and multi-component Fermi gases.

Acknowledgments

The author is grateful to J. Carlson for very useful discussions and critical comments on the manuscript. The research presented in this paper has been supported by the U.S. Department of Energy, Office of Nuclear Physics, the NUCLEI SciDAC program and by the LANL LDRD program. Computing time were made available by Los Alamos Open Supercomputing. This research used also resources of the National Energy Research Scientific Computing Center, which is supported by the Office of Science of the U.S. Department of Energy under Contract No. DE-AC02-05CH11231.

References

- [1] Giorgini S, Pitaevskii L P and Stringari S 2008 *Rev. Mod. Phys.* **80** 1215–1274
- [2] Zwierlein M W, Schirotzek A, Schunck C H and Ketterle W 2006 *Science* **311** 492
- [3] Partridge G B, Li W, Kamar R I, an Liao Y and Hulet R G 2006 *Science* **311** 503
- [4] Pilati S and Giorgini S 2008 *Phys. Rev. Lett.* **100** 030401
- [5] Lobo C, Recati A, Giorgini S and Stringari S 2006 *Phys. Rev. Lett.* **97** 200403
- [6] Bulgac A, Forbes M M and Schwenk A 2006 *Phys. Rev. Lett.* **97** 020402
- [7] Bulgac A and Forbes M M 2008 *Phys. Rev. Lett.* **101** 215301

- [8] Wille E, Spiegelhalder F M, Kerner G, Naik D, Trenkwalder A, Hendl G, Schreck F, Grimm R, Tiece T G, Walraven J T M, Kokkelmans S J J M F, Tiesinga E and Julienne P S 2008 *Phys. Rev. Lett.* **100** 053201
- [9] Spiegelhalder F M, Trenkwalder A, Naik D, Kerner G, Wille E, Hendl G, Schreck F and Grimm R 2010 *Phys. Rev. A* **81** 043637
- [10] Kohstall C, Zaccanti M, Jag M, Trenkwalder A, Massignan P, Bruun G M, Schreck F and Grimm R 2012 *Nature* **485** 615–618
- [11] Gezerlis A, Gandolfi S, Schmidt K E and Carlson J 2009 *Phys. Rev. Lett.* **103** 060403
- [12] Gubbels K B, Baarsma J E and Stoof H T C 2009 *Phys. Rev. Lett.* **103** 195301
- [13] Baarsma J E, Gubbels K B and Stoof H T C 2010 *Phys. Rev. A* **82** 013624
- [14] Baranov M A, Lobo C and Shlyapnikov G V 2008 *Phys. Rev. A* **78** 033620
- [15] Carlson J, Chang S Y, Pandharipande V R and Schmidt K E 2003 *Phys. Rev. Lett.* **91** 050401
- [16] Astrakharchik G E, Boronat J, Casulleras J and Giorgini S 2004 *Phys. Rev. Lett.* **93** 200404
- [17] Carlson J and Reddy S 2005 *Phys. Rev. Lett.* **95** 060401
- [18] Bulgac A, Drut J E and Magierski P 2006 *Phys. Rev. Lett.* **96**(9) 090404
- [19] Carlson J and Reddy S 2008 *Phys. Rev. Lett.* **100** 150403
- [20] Gandolfi S, Schmidt K E and Carlson J 2011 *Phys. Rev. A* **83** 041601
- [21] Carlson J, Gandolfi S, Schmidt K E and Zhang S 2011 *Phys. Rev. A* **84**(6) 061602
- [22] Forbes M M, Gandolfi S and Gezerlis A 2012 *Phys. Rev. A* **86**(5) 053603
- [23] Chang S Y, Pandharipande V R, Carlson J and Schmidt K E 2004 *Phys. Rev. A* **70** 043602
- [24] Morris A J, López Ríos P and Needs R J 2010 *Phys. Rev. A* **81** 033619
- [25] Forbes M M, Gandolfi S and Gezerlis A 2011 *Phys. Rev. Lett.* **106** 235303
- [26] Sorella S 2001 *Phys. Rev. B* **64** 024512
- [27] Vitali E, Arrighetti P, Rossi M and Galli D E 2011 *Molecular Physics* **109** 2855–2862
- [28] Carlson J, Gandolfi S and Gezerlis A 2012 *Progress of Theoretical and Experimental Physics* **2012** 01A209
- [29] Foulkes W M C, Mitas L, Needs R J and Rajagopal G 2001 *Rev. Mod. Phys.* **73**(1) 33–83
- [30] Ku M J H, Sommer A T, Cheuk L W and Zwierlein M W 2012 *Science* **335** 563
- [31] Gezerlis A and Carlson J 2008 *Phys. Rev. C* **77**(3) 032801
- [32] Gezerlis A and Carlson J 2010 *Phys. Rev. C* **81**(2) 025803
- [33] Huang K and Yang C N 1957 *Phys. Rev.* **105**(3) 767–775
- [34] Lee T D, Huang K and Yang C N 1957 *Phys. Rev.* **106** 1135–1145
- [35] Petrov D S, Salomon C and Shlyapnikov G V 2005 *J. Phys. B: At. Mol. Opt. Phys.* **38** S645
- [36] Tan S 2008 *Ann. Phys.* **323** 2952–2970
- [37] Tan S 2008 *Ann. Phys.* **323** 2971–2986
- [38] Tan S 2008 *Ann. Phys.* **323** 2987–2990
- [39] Navon N, Nascimbène S, Chevy F and Salomon C 2010 *Science* **328** 729–732
- [40] Kuhnle E D, Hu H, Liu X J, Dyke P, Mark M, Drummond P D, Hannaford P and Vale C J 2010 *Phys. Rev. Lett.* **105** 070402
- [41] Stewart J T, Gaebler J P, Drake T E and Jin D S 2010 *Phys. Rev. Lett.* **104** 235301
- [42] Enss T, Haussmann R and Zwerger W 2011 *Annals of Physics* **326** 770 – 796
- [43] Hoinka S, Lingham M, Fenech K, Hu H, Vale C J, Drut J E and Gandolfi S 2013 *Phys. Rev. Lett.* **110**(5) 055305
- [44] Kuhnle E D, Hoinka S, Hu H, Dyke P, Hannaford P and Vale C J 2011 *New Journal of Physics* **13** 055010
- [45] Veeravalli G, Kuhnle E, Dyke P and Vale C J 2008 *Phys. Rev. Lett.* **101**(25) 250403
- [46] Hoinka S, Lingham M, Delehay M and Vale C J 2012 *Phys. Rev. Lett.* **109**(5) 050403